AIP | Applied Physics Letters

Quantum transport of Au-S-S-Au nanoscale junctions

Jing-Xin Yu, Xiang-Rong Chen, Stefano Sanvito, and Yan Cheng

Citation: Appl. Phys. Lett. **100**, 013113 (2012); doi: 10.1063/1.3665614
View online: http://dx.doi.org/10.1063/1.3665614
View Table of Contents: http://apl.aip.org/resource/1/APPLAB/v100/i1
Published by the American Institute of Physics.

Quantum transport of Au-S-S-Au nanoscale junctions

Jing-Xin Yu,[1] Xiang-Rong Chen,[1,2,a)] Stefano Sanvito,[3,a)] and Yan Cheng[1,a)]
[1]*Institute of Atomic and Molecular Physics, College of Physical Science and Technology, Sichuan University, Chengdu 610064, China*
[2]*International Centre for Materials Physics, Chinese Academy of Sciences, Shenyang 110016, China*
[3]*School of Physics and CRANN, Trinity College, Dublin 2, Ireland*

(Received 29 August 2011; accepted 29 October 2011; published online 6 January 2012)

Transport in S_2 molecules sandwiched between Au electrodes is investigated with a combination of density functional theory and the non-equilibrium Green's function method. We consider four different configurations and find that their conductances are related to the details of the bonding geometry. When S_2 connects to pyramidal-shaped electrodes at the top site, the transmission is governed by a resonance and is strongly affected by the bias. In contrast, the transport of the remaining three configurations is through several closely spaced broad molecular orbitals, and the transmission coefficient is almost flat around the Fermi level. © *2012 American Institute of Physics*. [doi:10.1063/1.3665614]

The long envisioned possibility of trapping single molecules between metallic break junctions (MBJs) has become a reality only in the mid-nineties,[1–3] when the difficulties in establishing stable and reproducible molecule/electrode contacts have been overcome. At present, several experimental investigations demonstrate that diatomic molecules can form a molecular contact with metals such as Au, Ag, Pt, and Pd.[4,5] These contacts are stable enough to perform statistical MBJs transport experiments, where conductance histograms are collected over subsequent cycles of the junction breaking. Such experiments provide a fundamental understanding of the molecule/metal interaction and of the molecules' ability of transferring electrons. Theory has played a fundamental role in explaining existing experiments and in designing new ones.[6,7] In particular, quantum transport calculations based on accurate electronic structure theories have helped in directly correlating the electron transfer process to the details of the molecule/electrode interaction. In the spirit of using theoretical predictions ahead of experiments, here, we propose the investigation of S_2 in Au-based MBJs. Interestingly, although S is usually rather reactive, we find here that S_2 forms several stable molecular junctions, whose transport properties depend sensitively on the orientation of the molecule with respect to the electrodes. This is not the first time that molecular junctions can be made with reactive materials. For instance, although Pd absorbs H extremely efficiently, transport experiments have been successfully conducted for H_2 molecules sandwiched between Pd electrodes.[5] We wish to stress here that the agreement between theory and experiments for electron transport in these small molecules is usually good,[5–7] so that we expect that our theoretical predictions might find soon an experimental verification.

Sulphur is an ubiquitous element in molecular electronics as thiol is the mostly used chemical group for anchoring molecules to Au,[8–10] but still, the thiol chemistry on Au presents fascinating aspects.[11,12] In general, there are advantages and disadvantages in using S as linking group. On the one hand, the S-Au bond is strong, although the high surface mobility of Au may still result in thermally unstable junctions.[10] On the other hand, as thiol bonds to Au, it looses any useful subsequent chemical functionality so that little further chemical manipulation is possible. Such a disadvantage is overcome in S_n clusters that naturally bond to Au but still preserve a rich chemical activity. Note, however, that in general, devices made with molecules that remain reactive may be difficult to handle and their reproducibility may be low. Recently, we have studied the transport properties of S_9 clusters, which show strong bonding to Au and good conducting properties.[13] Here, we explore S_2, the end of the S_n series,[14] and compare the bonding structure, the conductance and the *I-V* curves of four different Au(100)-S_2-Au(100) molecular junctions as they are broken apart.[15]

The electronic structure and the transport properties have been calculated with the *ab initio* transport code SMEAGOL,[16] which combines the non-equilibrium Green's function[17] formalism with density functional theory.[18] We use the Perdew-Zunger local-density approximation[19] to the exchange-correlation functional and a double-zeta plus polarization basis set. Nonlocal scalar-relativistic Troullier-Martins pseudopotentials are generated from the configurations: Au ($5d^{10}6s^1$), S ($3s^2 3p^4$). Periodic boundary conditions are applied in the plane orthogonal to the transport direction with four *k*-points in the two-dimensional Brillouin zone. A *k*-grid sampling of $2 \times 2 \times 100$ for the Au electrodes is employed, together with a mesh cut-off of 200 Ry. We consider 128 real and 50 complex energy points when integrating the Green function.

The scatterng region includes the S_2 molecule and, respectively, seven and six Au atomic layers, (001)-oriented and with 3×3 cross-section, at each side of the junction. Four S_2 anchoring geometries are investigated (see insets of Fig. 1): (a) S_2 connected to pyramical-shaped electrodes at the top site with the molecular axis parallel to the transport direction (*z*-axis), (b) same as in (a) but with the molecular axis perpendicular to *z*, (c) S_2 connected to pyramical electrodes at the hollow site to the left and at the top site to the right (molecular axis parallel to *z*), and (d) S_2 connected to two hollow sites with the molecular axis parallel to *z*. The most stable structures are found by geometry relaxation with

a)Authors to whom correspondence should be addressed. Electronic addresses: x.r.chen@qq.com, sanvitos@tcd.ie, and ycheng@scu.edu.cn.

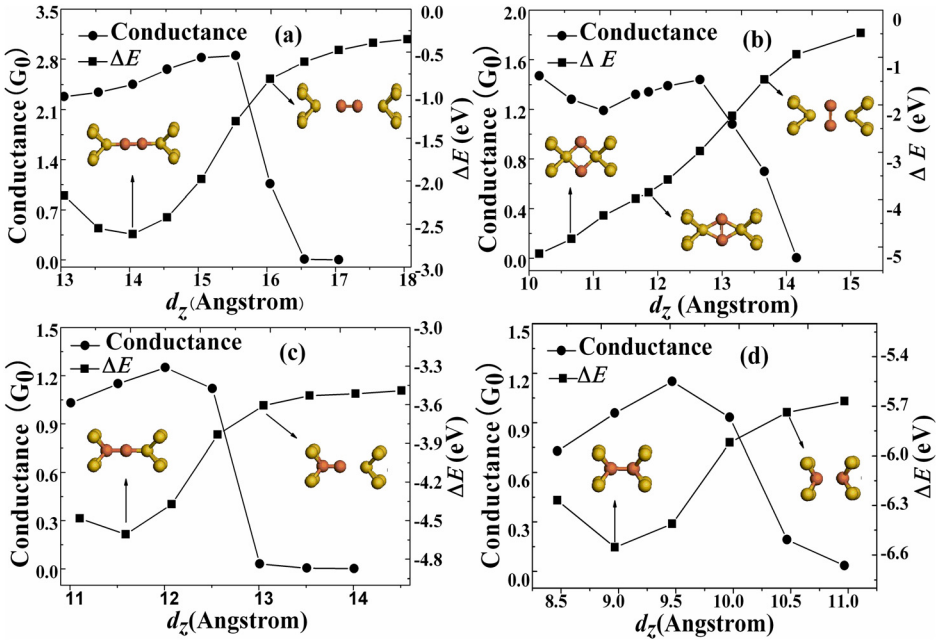

FIG. 1. (Color online) Conductance (circles and left-hand side axis) and cohesion energy (squares and right-hand side axis) for the four configurations investigated as a function of distance d_Z between the two Au (100) electrodes: (a) top-top parallel configuration, (b) top-top perpendicular configuration, (c) top-hollow configuration, and (d) hollow-hollow configuration. In the insets, we present the geometrical structures of the junctions at different electrodes' elongations.

the bulk Au leads kept fixed.[15] The ground state energy is calculated as a function of the distance d_z between the outer Au layers, i.e., we simulate a slow junction breaking process.

Fig. 1 presents the cohesion energy, $\Delta E = E(\text{Au electrode} + S_2) - E(S_2) - E(\text{Au electrode})$, as a function of d_z for all the configurations. This is the energy of the junction (S_2 plus the Au atoms in scattering region) relative to the sum of the energy of S_2 in the gas phase and that of the Au layers included in the scattering region. We find that, for (a), (c), and (d), $\Delta E(d_z)$ is a parabola with minima located, respectively, at the equilibrium distances, $d_{z,eq} = 14.049$ Å, $d_{z,eq} = 11.509$ Å, and $d_{z,eq} = 8.969$ Å. Thus, $d_{z,eq}$ describes the optimal device, which is the device that will naturally form if the electrodes are free to relax. For (a), the Au-S bond-length, d_{S-Au}, is 2.36 Å, while it is, respectively, 2.63 Å at the hollow site and 2.37 Å at the top site for (c). Finally, for (d), $d_{S-Au} = 2.61$ Å at the hollow site. At variance with (a), (c), and (d), there is no local minimum in $\Delta E(d_z)$ for (b), which changes as follows as the electrodes are pulled apart. For small d_{S-Au} (compression), the electrodes' apexes sit in the middle of the S-S bond, which is stretched. As the MBJ is pulled, the S-S bond-length gets compressed while d_{S-Au} increases. We find that for $d_z = 11.86$ Å, the S-S bond-length is close to the experimental value of 1.889 Å (Ref. 20) and $d_{S-Au} \sim 2.54$ Å. Overall, for all the configurations, the obtained d_{S-Au} is consistent with previous literature.[8,13,21]

Together with $\Delta E(d_z)$, we also calculate the conductance as a function of distance d_z (also Fig. 1). This is evaluated by using the Landauer formula $G = G_0\ T(E_F;\ V = 0)$, where $G_0 = 2e^2/h$ is the conductance quantum and $T(E_F;\ V = 0)$ is the transmission coefficient at zero−bias ($V = 0$) calculated at the Fermi level, E_F. In general, for all the configurations, we find that G increases as the contact is pulled apart. This is a similar to what happens to a single S atom and demonstrates the sensitivity of the conductance to the local atomic re-arrangement of the contact region.[22] Going into more details, we observe that for (a), G increases from $2.28G_0$ to $2.85G_0$ as d_z goes from 13 Å to 15.5 Å. Then, for $d_z > 15.5$ Å, the Au-S bond breaks, the junction snaps, and G jumps abruptly from $\sim 2.85G_0$ to $\sim 1.06G_0$ ($d_z \sim 16$ Å) and then remains small for any larger d_z. A similar trend is observed for (c) and (d) with G increasing monotonically [from $1.03G_0$ to $1.25G_0$ for (c) and from $0.73G_0$ to $1.15G0$ for (d)] until the bond breaking point. Finally, (b) behaves differently as G first decreases from $1.47G_0$ to $1.19G_0$ for d_z going from ~ 10 Å to ~ 11 Å and then it increases until the Au-S bond breaking point.

The differences in conductance between the anchoring geometries can be understood by analysing the transmission function $T(E;V)$ and the orbital resolved projected density of states (PDOS) of the Au-S_2-Au junctions at the equilibrium distance (Fig. 2). For (a), E_F of Au is located at a peak in the transmission function where it pins. Thus, $T(E_F;0)$ is dominated by a resonance corresponding to the energy of the highest occupied molecular orbital (HOMO), ε_{HOMO}. This provides a large G so that (a) has the largest transmission among all the junctions. Such a highly conductive transport channel is mainly formed by the S p_x and p_y orbital, with an almost negligible contribution from p_z (not shown; note that p_z points towards the electrodes). Therefore, for (a), the transport is via π–conjugation across the junction. In fact, the PDOS also reveals that the S_2/electrodes electron coupling is through S p_x and p_y and the Au s, d_{xz}, d_{yz}.

In (b), E_F is located just above the molecule HOMO, but this time G is no longer due to the S p_x and p_y orbitals but to the coupling between S p_z and Au d_{xz}, d_{yz}, reflecting the 90° rotation of the molecule when going from (a) to (b). Note that, although in a tight-binding picture, there is no hopping integral between p_z and d_{xz}, d_{yz} if the bond axis is along the z direction; this is true here where the bond direction forms an angle with z. Still, the electronic coupling remains weak. For this reason, the HOMO contributes little to G. For the remaining (c) and (d) configurations, where S_2 binds at least at one side at the hollow site, the electronic coupling is considerably stronger than in (a). This affects the S_2 HOMO

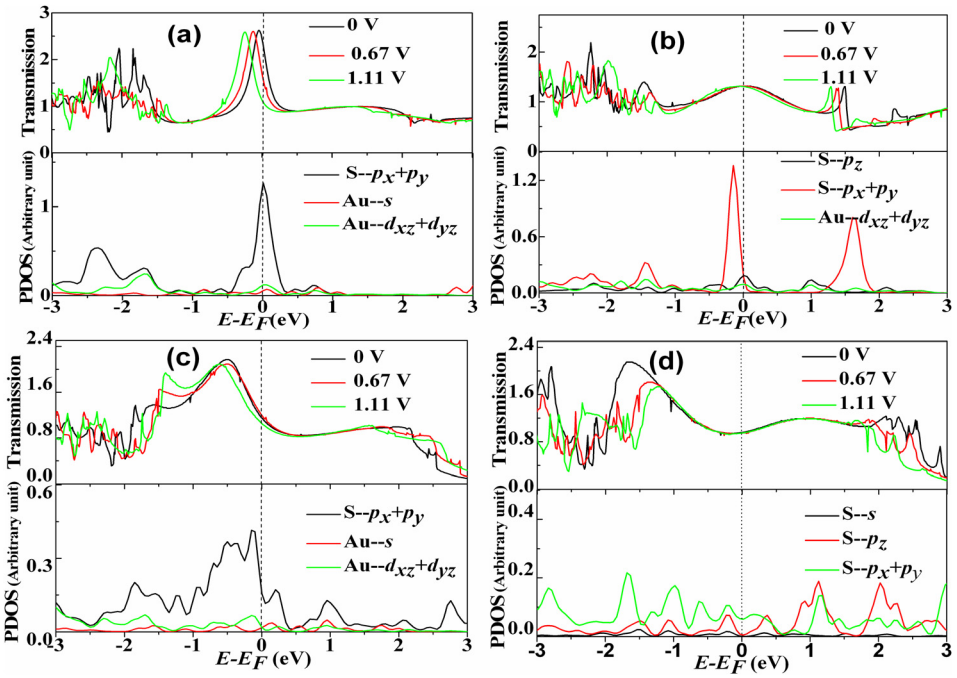

FIG. 2. (Color online) Transmission coefficient as a function of energy (top panels) and PDOS (lower panels) for an S_2 molecule attached to gold (100) electrodes: (a) top-top parallel configuration, (b) top-top perpendicular configuration, (c) top-hollow configuration, and (d) hollow-hollow configuration.

broadening to a point where it becomes indistinguishable in the PDOS. As a consequence, there is no resonance at E_F, but instead, $T(E)$ is flat and featureless. In all cases, the conductance is around 1 G_0 at E_F, which is what is expected for a single *s* channel.

We now look at the dependence of $T(E;V)$ upon bias (upper panels of Fig. 2). In this case, (a) behaves completely differently from all the others. In fact for (a), we observe a significant drift of the HOMO resonance to lower energies as V is increased. Such a drift moves the HOMO away from the E_F. However, the transmission peak does not leave the bias window, and therefore, the current (see later) and the conductance remain relatively large. In contrast, for the configurations (b), (c), and (d), little happens to $T(E;V)$ around E_F as V is increased. This is what expected from a metallic-like junction.

The dependence of $T(E; V)$ on bias sets the shape of the *I-V* characteristics (Fig. 3). In general, there is little difference between the four anchoring geometries, as one may expect from devices showing metallic-like transmission with zero-bias conductance around G_0 and featureless $T(E; V)$ for $E \sim E_F$. Thus, all the *I-V* are linear and featureless. Still, some qualitative differences exist. For instance, (a) shows a clear slope change in the *I-V* for $|V| > 0.25$ V. This corresponds to the saturation of the contribution to the current originating from the HOMO. Since other junctions do not have a distintive peak contributing $T(E_F)$, they do not display any slope change. The only other exception is for configuration (c) which displays an asymmetric *I-V* curve, with the conductance (dI/dV) being larger for $V > 0$ than for $V < 0$. Such an asymmetry is expected and originates from the asymmetric anchoring geometry and from a slightly different molecule charging for the two bias polarities.

In conclusion, we have presented a density functional theory and non-equilibrium Green's function (DFT-NEGF) study of the electron transport of four geometrically different S_2/Au MBJs. In general, all the junctions show large zero-bias conductance and linear *I-V* curves. This demonstrates the rather strong electronic coupling between S_2 and the electrodes, which manifests itself in the large and featureless $T(E;V=0)$ around E_F. The only exception is when S_2 molecule is parallel to the transport direction and attaches at the top sites, (a). In this case, the transmission originates most from a narrow peak in the PDOS corresponding to the molecule HOMO. Such a peak is responsible for the low bias conductance and for a change in slope in the *I-V* curve at $|V| > 0.25$ V.

As S is the most popular linking element for molecules on Au, the relevance of our calculations goes beyond the determination of the conductance of S_2. In particular, we have demonstrated that the S π–bonding can sustain a very large current. It is then expected that π–conjugated molecules linked to Au by S may exhibit large transmission.

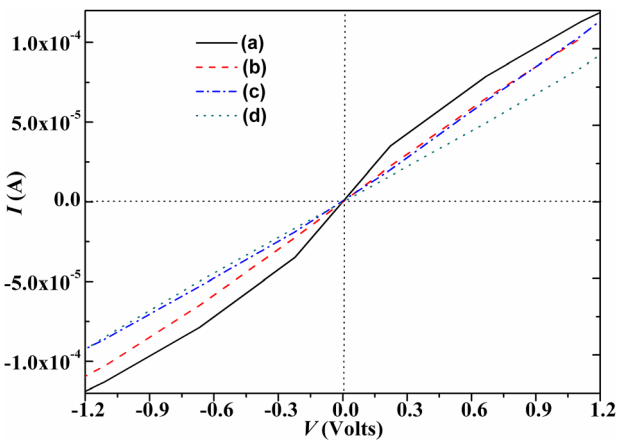

FIG. 3. (Color online) *I-V* curves calculated for four configurations between the S_2 cluster and the electrodes at the equilibrium positions: (a) top-top parallel configuration, (b) top-top perpendicular configuration, (c) top-hollow configuration, and (d) hollow-hollow configuration.

Furthermore, we anticipate that it will be possible to verify experimentally our calculations by either MBJs or by scanning tunnel microscopy (STM) experiments. In the case of STM, these may also reveal important information about catalytic processes of S on Au.

We thank the support of the National Natural Science Foundation of China (11174214) and the SRFDP (20090181110080). SMEAGOL (SS) is sponsored by Science Foundation of Ireland (07/IN.1/I945) and CRANN.

[1]M. A. Reed, C. Zhou, C. J. Muller, T. P. Burgin, and J. M. Tour, Science **278**, 252 (1997).
[2]R. L. McCreery, Chem. Mater. **16**, 4477 (2004).
[3]A. Nitzan and M. A. Ratner, Science **300**, 1384 (2003).
[4]R. H. M. Smit, Y. Noat, C. Untiedt, N. D. Lang, M. C. van Hemert, and J. M. van Ruitenbeek, Nature (London) **419**, 906 (2002).
[5]S. Csonka, A. Halbritter, G. Mihaly, O. I. Shklyarevskii, S. Speller, and H. van Kempen, Phys. Rev. Lett. **93**, 016802 (2004).
[6]V. M. García-Suárez, A. R. Rocha, S. W. Bailey, C. J. Lambert, S. Sanvito, and J. Ferrer, Phys. Rev. B **72**, 045437 (2005).
[7]K. H. Khoo, J. B. Neaton, H. J. Choi, and S. G. Louie, Phys. Rev. B **77**, 115326 (2008).
[8]C. Toher and S. Sanvito, Phys. Rev. B **77**, 155402 (2008); Phys. Rev. Lett. **99**, 056801 (2007).
[9]S. Martín, D. Zsolt Manrique, V. M. García-Suárez, W. Haiss, S. J. Higgins, C. J. Lambert, and R. J. Nichols, Nanotechnology **20**, 125203 (2009).
[10]G. S. Tulevski, M. B. Myers, M. S. Hybertsen, M. L. Steigerwald, and C. Nuckolls, Science **309**, 591 (2005).
[11]T. Sato, D. Brown, and B. F. G. Johnson, Chem. Commun. **11**, 1007 (1997).
[12]M. Yu, N. Bovet, C. J. Satterley, S. Bengió, K. R. J. Lovelock, P. K. Milligan, R. G. Jones, D. P. Woodruff, and V. Dhanak, Phys. Rev. Lett. **97**, 166102 (2006).
[13]J. X. Yu, X. R. Chen, and S. Sanvito, Phys. Rev. B **82**, 085415 (2010).
[14]K. Raghavachari and J. S. Binkley, J. Chem. Phys. **87**, 2191 (1987).
[15]R. B. Pontes, A. R. Rocha, S. Sanvito, A. Fazzio, and A. J. Roque da Silva, ACS Nano **5**, 795 (2011).
[16]A. R. Rocha, V. M. Garcia-Suarez, S. Bailey, C. Lambert, J. Ferrer, and S. Sanvito, Phys. Rev. B **73**, 085414 (2006); I. Rungger and S. Sanvito, Phys. Rev. B **78**, 035407 (2008).
[17]L. P. Kadanoff and G. Baym, *Quantum Statistical Mechanics* (Benjamin-Cummings, New York, 1962).
[18]W. Kohn and L. Sham, Phys. Rev. **140**, A1133 (1965).
[19]J. P. Perdew, Phys. Rev. B **33**, 8822 (1986).
[20]E. Q. Geoffrey, F. S. Henry III, and J. M. Colin, J. Am. Chem. Soc. **112**, 8719 (1990).
[21]A. Cossaro, R. Mazzarello, R. Rousseau, L. Casalis, A. Verdini, A. Kohlmeyer, L. Floreano, S. Scandolo, A. Morgante, M. L. Klein, and G. Scoles, Science **321**, 943 (2008).
[22]I. S. Kristensen, D. J. Mowbray, K. S. Thygesen, and K. W. Jacobsen, J. Phys.: Condens. Matter **20**, 374101 (2008).